

# 3B.3 Isentropic descent beneath the Saharan Air Layer and its impact on tropical cyclogenesis

Michael Diaz

## 1 Introduction

Although many Atlantic tropical cyclones originate from African Easterly Waves (AEW), very few AEWs actually generate tropical cyclones (Pasch et al. [1998]). Recently, there has been increased interest in the effects of the Saharan Air Layer (SAL) on AEWs and tropical cyclogenesis. Some studies suggest that the SAL can encourage tropical cyclogenesis by amplifying AEWs through baroclinic energy conversion (Karyampudi and Pierce [2002], Karyampudi and Carlson [1988]), whereas most recent studies suggest that it inhibits tropical cyclogenesis by introducing dry, stable air at low levels and increasing wind shear (Dunion and Velden [2004]). One recent study even finds that the SAL has little significant impact on tropical cyclogenesis (Braun). Extending earlier work on the SAL's influence on AEWs, the focus of our research is another potentially important consequence of the SAL which has thus far received little treatment; it induces strong isentropic descent north of AEWs.

The objective of this study is to describe this process and how it may impact AEWs. Unlike earlier studies which emphasize the negative influence of the dry air within the SAL on convection, our results suggest that much of the dry air within AEWs at lower levels is actually of mid-latitude origin; isentropic descent beneath the SAL brings this dry, mid-latitude air from aloft to lower levels. This process does not necessarily require direct contact of the SAL with the AEW. We hypothesize that this dry air and the extent to which it moistens plays a role in tropical cyclogenesis from AEWs.

## 2 Objective

Using a large sample of AEWs, we estimate the fraction of airmass within AEWs which has a history of isentropic descent along the northwest African coast. We then examine which regions of

the AEW tend to contain this airmass and determine whether or not it is detrimental to AEW convection and future tropical cyclogenesis. We also investigate the history of this airmass before it reaches AEWs and how it impacts AEW spatial structure. For brevity, we will refer to it as "air with history of Isentropic Descent" (ID).

## 3 Methods

For our analysis, we employ the  $1.0^\circ \times 1.0^\circ$  Global Forecast System (GFS) Final (FNL) analyses from 2000 to 2008. In order to sample a large number of AEWs in the eastern Atlantic which could serve as tropical cyclone precursors, we develop an automated vortex identification algorithm which uses maxima in curvature vorticity to locate AEWs. For each identified AEW, we perform a six day isentropic back trajectory analysis in order to identify each AEW's airmass source regions. Back trajectories are started every 1 K within a 299-309 K vertical layer and every  $0.5^\circ$  within a  $5^\circ \times 5^\circ$  horizontal box centered on the maximum in curvature vorticity for each system. We focus on this vertical layer, because additional analysis shows that AEWs contain negligible ID above 309 K. To estimate the prevalence of ID in AEWs, we calculate the fraction of trajectories with a history of isentropic descent within a 300 km radius of the circulation center for all of the identified cases. We deem the air mass within this relatively small radius to be important, since tropical cyclogenesis requires convection to be collocated with the low level circulation center and 600 km is a typical diameter of a tropical cyclone. Altering this value by about 100 km has little effect on our general conclusions.

To assess how ID affects AEWs and their probability of tropical cyclogenesis, we perform composite analyses of AEWs and group them into "developing" and "non-developing" cases based on whether they formed a tropical cyclone east of

60°W. We then relate these composites and subsequent tropical cyclogenesis to the fraction of ID within the AEW circulation. The procedure to generate composites for AEWs is to use the curvature vorticity maxima identified by the aforementioned algorithm as a center point and overlay GFS grids in a 20° x 20° box centered on these maxima and average the grids. The goal is to determine the structure of an AEW based on the fraction of ID ingested into its circulation. We test the statistical significance of the differences between developing and non-developing systems by calculating p-values. Since many of our distributions are highly skewed, we used Monte Carlo simulations to determine these p-values.

To further examine the dynamics and history of this air mass, an average trajectory was constructed by binning each point along the trajectory according to latitude and averaging all points along a given latitude. Constraining the trajectories to a narrow region along the African coast forces them to follow a similar path and thus justifies this averaging technique.

## 4 Climatology

To illustrate the process of isentropic descent, we plot mean July through September pressure, winds, and mixing ratio on the 303 K isentropic surface (Fig. 1). Offshore and along the African coast, there is a strong isentropic pressure gradient, which is a manifestation of the strong temperature gradient between the hot Sahara and the much cooler marine air mass. Consistent with this strong gradient, the 303 K isentrope dips sharply toward the surface near the African coast. The SAL is clearly evident between 10°N and 25°N in the eastern Atlantic, where the 303 K isentrope dips toward the surface. From this analysis, the cause of the isentropic descent in this region becomes clear; mid-latitude westerly winds interacting with the northern fringe of the SAL are forced by the strongly sloping isentropes to turn southward via thermal wind balance and rapidly descend. Since the average mid-latitude westerly flow at 303 K is located between about 800 mb and 750 mb and has mixing ratios of less than 6 g/kg, this pattern provides a nearly continuous flow of dry mid-latitude air southward along the African coast, beneath the SAL, and into the tropics.

As a further illustration of this process, we ex-

amine average 925 mb mixing ratio in the eastern Atlantic (Fig. 2). The most striking feature of this analysis is the elongated bull’s eye of reduced mixing ratios offshore along the African coast. This pattern is somewhat counterintuitive, since the air above the ocean is drier than the air above the desert. Since the winds in this region are primarily northerly and mixing ratios of less than 6 g/kg occur about 600 km west of similar values in the Sahara, this dryness does not seem related to the Sahara’s dryness. Based on Fig. 1, the source of this dry air is in the mid-latitudes, and it is brought to low levels by isentropic descent beneath the SAL. The driest air at 925 mb occurs between 20°N and 27°N, where the isentropes dip closest to the surface.

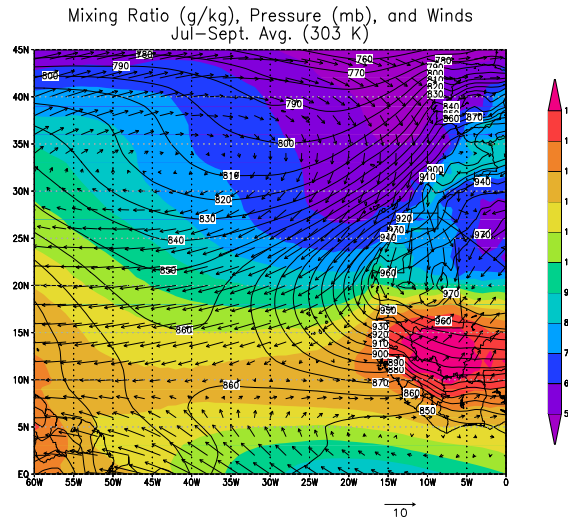


Figure 1: Average pressure (mb), mixing ratio (g/kg), and winds on the 303 K isentropic surface, using GFS analyses from 2000 to 2008 during July, August, and September

## 5 Analysis

### 5.1 Probability of Tropical Cyclogenesis

We hypothesize that entrainment of ID is detrimental to AEW convection and the probability that an AEW will undergo tropical cyclogenesis. To test this hypothesis, we compare the characteristics of developing and non-developing AEWs (Tab. 1) with respect to the fraction of ID contained within their circulation. The results of this analysis sug-

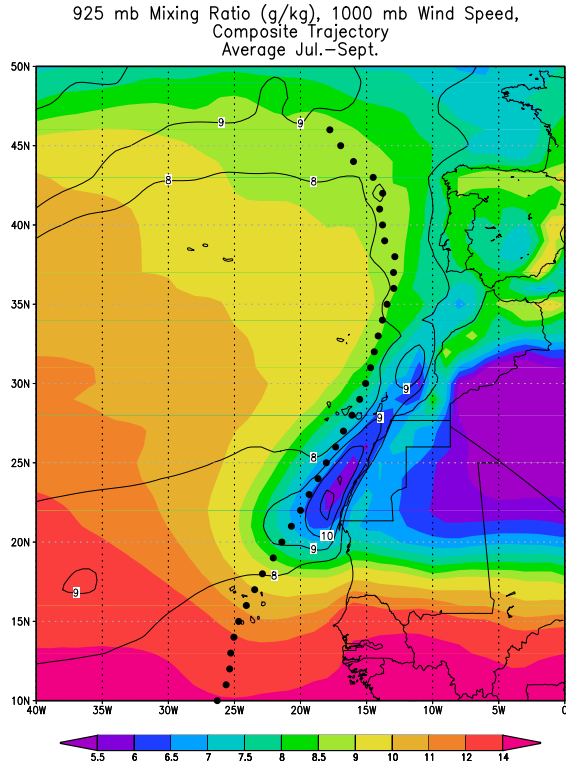


Figure 2: Composite 301 K trajectory, average July-September 925 mb mixing ratio (g/kg), and average 1000 mb wind (m/s). The color bar for mixing ratio has smaller intervals at lower values to emphasize dry air and the wind speed is contoured above 8 m/s.

Table 1: Summary statistics for all cases including the average latitude, average and median fraction of trajectories from ID, and total number of cases in each category.

	All	July	Aug.	Sept.
All Cases				
Avg. Lat.	11.79	12.21	12.54	10.57
Avg. %	69.24	78.87	74.61	54.41
Med. %	76.2	93.25	80.4	50.5
Total Cases	191	58	70	63
Developing				
Avg. Lat.	11.58	11	11.78	11.55
Avg. %	57.02	58.74	58.04	55.8
Med. %	50.5	70.1	55.65	49.95
Total Cases	45	5	18	22
Non-Developing				
Avg. Lat.	11.86	12.32	12.81	10.05
Avg. %	73.01	80.76	80.35	53.66
Med. %	84.45	94.8	90.7	50.5
Total Cases	146	53	52	41

gest that ID negatively impacts tropical cyclogenesis, with developing cases having an average of 73% of ID within their circulation, and developing cases with only 57%. With a p-value of 0.01, this difference seems robust. Since our distribution is strongly skewed toward higher fractions of ID, using the median as a comparison yields even larger differences, with developing cases having a value of 85% and non-developing 50%. However, breaking the cases down by month reveals that ID may be effective at inhibiting tropical cyclogenesis only during July and August, with little effect during September. Additional analysis (not shown) suggests that rapidly warming sea surface temperatures in August and September counteract the dry air through increased moisture fluxes.

## 5.2 Trajectory Composites

For a more detailed investigation of the process of isentropic descent along the African coast and how it impacts AEWs, we use the trajectory data generated for all AEW cases to construct composite trajectories of height (Fig. 3) and moistening rates (Fig. 4). A plan view map of this trajectory is shown in Fig. 2.

From Fig. 3, it is clear that most of the isentropic descent occurs between about 35°N and

46°N, where air parcels on average drop approximately 1 km. Since most of the trajectories still remain above 1 km north of 35°N, little moistening occurs, with mixing ratio increasing by only about 0.25 g/kg per day (Fig. 4). As air parcels travel from 35°N and 22°N, they continue to descend beneath the thickening SAL, but at a slower rate than previously. The plot of 925 mb mixing ratio with composite trajectory overlaid (Fig. 2) clearly shows the impact of this descent as an elongated region of lower mixing ratios immediately offshore. Continued descent squeezes the isentropes into a thin layer near the surface and leads to extremely high low level static stability (Fig. 3). As they descend to their lowest altitude near 22°N, their rate of moistening rapidly increases to a maximum near 22°N (Fig. 4). This moistening is a function of height, as 301 K parcels moisten at about 2.5 g/kg per day at 22°N and 307 K parcels at about 1.5 g/kg. Once south of 22°N, the overlying SAL becomes thinner and air parcels consequently begin a slow ascent or remain at the same level (Fig. 3).

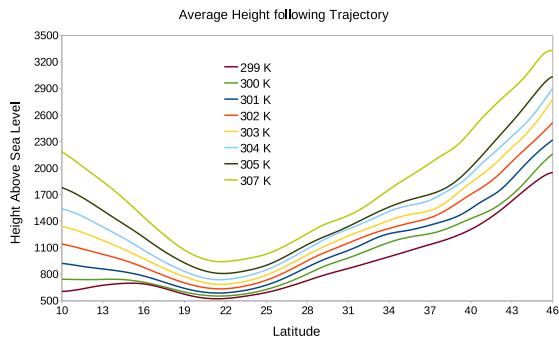


Figure 3: Height averaged along composite trajectory.

### 5.3 Frequency of ID within AEWs

We now examine the frequency at which different parts of an AEW circulation contain ID. The frequency of ID is calculated at each location within the 301-304 K layer at which a back trajectory begins (i.e. every 0.5° and every 1 K) within the 5° x 5° boxes centered on each AEW. For each grid point, we calculate the percent of cases which contain ID and average this percent over all four levels within the 301-304 K layer. The results of this procedure are plotted in Fig. 5, which shows the

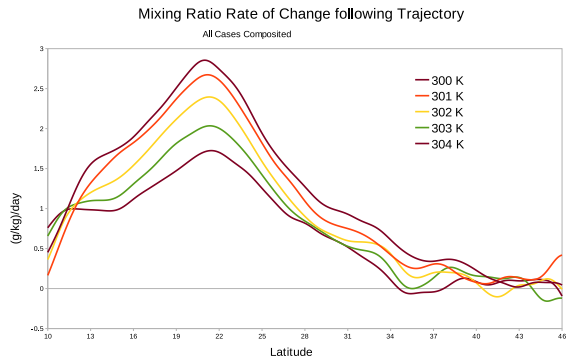


Figure 4: Mixing ratio rate of change averaged along composite trajectory.

frequency at which ID occurs within an AEW circulation overlaid with the wind velocity field averaged for all cases. The distribution of the frequency of this air mass within an AEW circulation reveals a clear pattern; higher frequencies occur over the northwestern region and lower frequencies over the southeastern region (Fig. 5). This pattern should be expected, since northerly winds ahead of the circulation are more likely to have originated from the north, where ID originates.

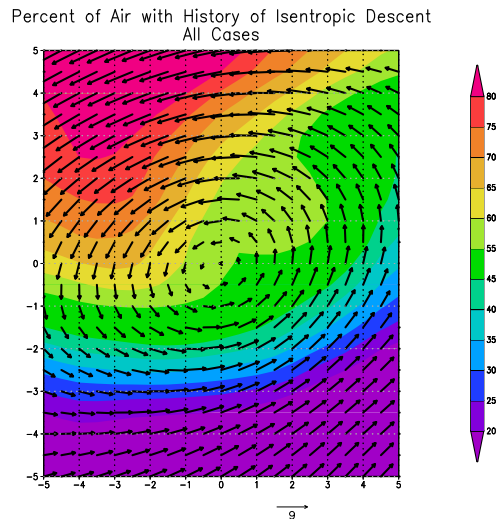


Figure 5: Frequency at which different regions of the circulation contain air mass with a history of isentropic descent for all AEW cases.

## 5.4 Field Composites

To investigate how ID impacts AEWs, we compare composite meteorological fields for our cases. We separate our cases by the fraction of ID contained within a 300 km radius of the circulation center and place them into three categories, 0-40%, 40-80%, and 80-100%. The intervals are not evenly divided, since a comparatively large number of cases fall into the 80-100% category. For the composite, we view the 303 K mixing ratio, 303 K winds, and 500 mb vertical velocity.

The 80-100% composite AEW (Fig. 6) is nearly devoid of convection within 200 km of its circulation center, but contains a broad band of convection well to its south. Considering that the center of our cases averages near 12°N, this convection would typically be centered near 6°N, which places it within the intertropical convergence zone (ITCZ). The dry air associated with ID is clearly apparent in the northwest quadrant. Near the center, ID and moister air from the south are wrapping around each other cyclonically. In the 40-80% composite (Fig. 7), there is a definite northward shift in the convection and it now lies directly over the circulation center. However, it still has a southward bias as the dry air from ID seems to be eroding the northern edge of the convection ahead of the circulation. Nevertheless, in comparison with the 80-100% composites, this composite seems much more likely to become a tropical cyclone, since the convection is collocated with the circulation center. The 0-40% composite (Fig. 8) follows the same trend; convection shifts northward and appears stronger and less dry air from ID appears in the northwestern quadrant. Note that 16% of 92 cases in the 80-100% category undergo tropical cyclogenesis, compared with 26% of 61 cases in the 40-80% category, and 37% of 38 cases in the 0-40% category. Thus, the fraction of ID within an AEW circulation appears to be at least one of the factors influencing tropical cyclogenesis from AEWs.

## 6 Synthesis

Our analysis confirms that the SAL forces isentropic descent in the northeastern Atlantic near the northwest African coast. The extremely high potential temperature of the overlying SAL forces the underlying isentropes downward and thus causes the northerly flow on the eastern flank of the Azores

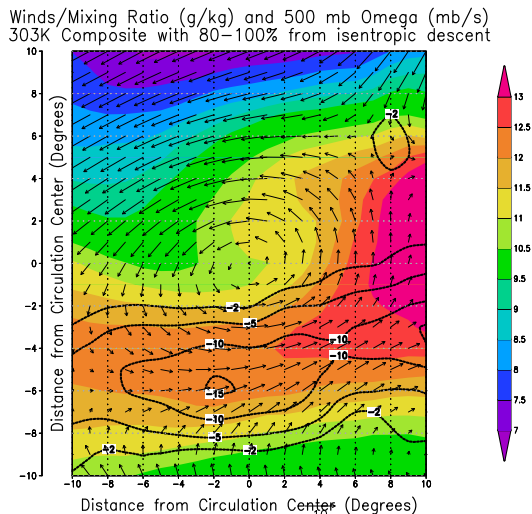


Figure 6: Composite 303 K mixing ratio (g/kg) (shaded), 500 mb vertical velocity (mb/day) (contoured), and 303 K winds (vectors) for cases with 80-100 % of their airmass with a history of isentropic descent.

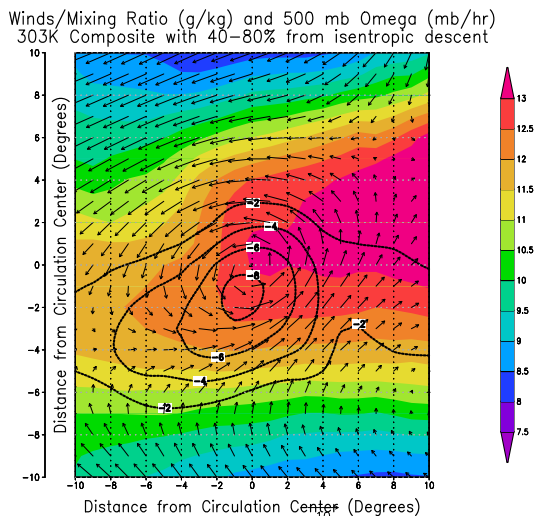


Figure 7: Same as Fig., but for 40-80%.

Winds/Mixing Ratio (g/kg) and 500 mb Omega (mb/hr)  
303K Composite with 0-40% from isentropic descent

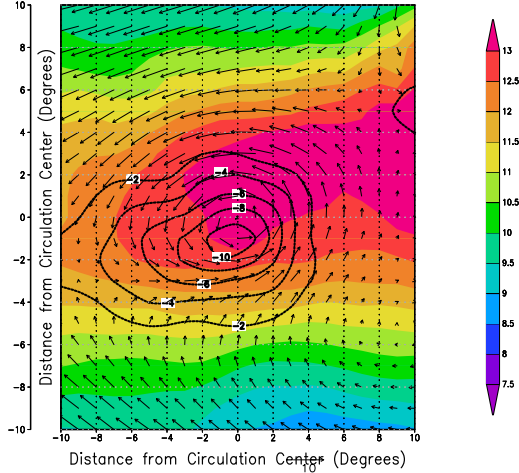


Figure 8: Same as Fig., but for 0-40%.

High to descend along the isentropes. One can visualize this descent as northerly flow from the mid-latitudes undercutting the SAL. This strong and persistent descent brings extremely dry air from aloft in the middle latitudes to low levels in the tropical eastern Atlantic.

We have also determined that AEWs exiting the African continent ingest a significant fraction of this airmass, which we have labeled ID, into their circulation and that it is detrimental to their convection and future tropical cyclogenesis, since it places extremely dry air at low levels and is often associated with high static stability. One can view the interaction between AEWs and ID as a multistage process. AEWs entering the eastern Atlantic tend to have a low level cyclonic circulation near 850 mb. Upon leaving the African continent, the northerly flow ahead of their circulation joins with the persistent northerly flow along the northwest African coast north of 20°N. This process brings dry air from the mid-latitudes into the AEW circulation and may suppress the convection within the AEW and reduce its probability of tropical cyclogenesis.

## 7 Acknowledgements

I would like to thank my collaborators on this work, Anantha Aiyer and Fredrick Semazzi, for their support. This research was funded under NOAA Grant NA06OAR4810187 and NSF Grant ATM-0847323.

## References

- Scott A. Braun. Re-evaluating the role of the saharan air layer in atlantic tropical cyclogenesis and evolution. *Monthly Weather Review*. doi: 10.1175/2009MWR3135.1.
- Jason P. Dunion and Christopher S. Velden. The impact of the saharan air layer on atlantic tropical cyclone activity. *Bulletin of the American Meteorological Society*, 85:353–365, 2004.
- V. Mohan Karyampudi and Toby N. Carlson. Analysis and numerical simulations of the saharan air layer and its effect on easterly wave disturbances. *Journal of the Atmospheric Sciences*, 45 (21):3102–3136, 1988.
- V. Mohan Karyampudi and Harold F. Pierce. Synoptic-scale influence of the saharan air layer on tropical cyclogenesis over the eastern atlantic. *Monthly Weather Review*, 130:3100–3128, 2002.
- Richard J. Pasch, Lixion A. Avila, and Jiann-Gwo Jiing. Atlantic tropical systems of 1994 and 1995: A comparison of a quiet season to a near-record-breaking one. *Monthly Weather Review*, 126: 1106–1123, 1998.